Health, 2024, 16, 856-871
https://www.scirp.org/journal/health
ISSN Online: 1949-5005
ISSN Print: 1949-4998

Brain Functional Network Changes in Patients with Poststroke Cognitive Impairment Following Acupuncture Therapy

Ran Wang[1,2*], Nian Liu[1*], Hao Xu[1], Peng Zhang[1], Xiaohua Huang[1], Lin Yang[1#], Xiaoming Zhang[1]

[1]Science and Technology Innovation Center, Interventional Medical Center, Department of Radiology, Affiliated Hospital of North Sichuan Medical College, Nanchong, China
[2]Department of Radiology, Sichuan Province Orthopedic Hospital, Chengdu, China
Email: #linyangmd@163.com

How to cite this paper: Wang, R., Liu, N., Xu, H., Zhang, P., Huang, X.H., Yang, L. and Zhang, X.M. (2024) Brain Functional Network Changes in Patients with Poststroke Cognitive Impairment Following Acupuncture Therapy. *Health*, **16**, 856-871.
https://doi.org/10.4236/health.2024.169061

Received: August 25, 2024
Accepted: September 24, 2024
Published: September 27, 2024

Abstract

Background: The mechanisms by which acupuncture affects poststroke cognitive impairment (PSCI) remain unclear. **Objective:** To investigate brain functional network (BFN) changes in patients with PSCI after acupuncture therapy. **Methods:** Twenty-two PSCI patients who underwent acupuncture therapy in our hospital were enrolled as research subjects. Another 14 people matched for age, sex, and education level were included in the normal control (HC) group. All the subjects underwent resting-state functional magnetic resonance imaging (rs-fMRI) scans; the PSCI patients underwent one scan before acupuncture therapy and another after. The network metric difference between PSCI patients and HCs was analyzed via the independent-sample *t* test, whereas the paired-sample *t* test was employed to analyze the network metric changes in PSCI patients before vs. after treatment. **Results:** Small-world network attributes were observed in both groups for sparsities between 0.1 and 0.28. Compared with the HC group, the PSCI group presented significantly lower values for the global topological properties (γ, Cp, and Eloc) of the brain; significantly greater values for the nodal attributes of betweenness centrality in the CUN. L and the HES. R, degree centrality in the SFGdor. L, PCG. L, IPL. L, and HES. R, and nodal local efficiency in the ORBsup. R, ORBsupmed. R, DCG. L, SMG. R, and TPOsup. L; and decreased degree centrality in the MFG. R, IFGoperc. R, and SOG. R. After treatment, PSCI patients presented increased degree centrality in the LING.L, LING.R, and IOG. L and nodal local efficiency in PHG. L, IOG. R, FFG. L, and the HES. L, and decreased betweenness centrality in the PCG. L and CUN. L, degree centrality in the ORBsupmed. R, and nodal local efficiency in ANG. R. **Conclusion:** Cognitive decline in PSCI patients may

*Co-first authors.
#Corresponding author.

be related to BFN disorders; acupuncture therapy may modulate the topological properties of the BFNs of PSCI patients.

Keywords

Cognitive Decline, Poststroke Cognitive Impairment, Functional Magnetic Resonance Imaging, Brain Functional Network, Graph Theoretical Analysis

1. Introduction

Poststroke cognitive impairment (PSCI) is a very common problem among individuals who experience stroke that severely impacts their activities of daily living while imposing heavy burdens on society and families [1] [2]. Many studies have shown that acupuncture has positive effects on PSCI [3]-[14]. Advances in imaging technologies have provided new approaches, including resting-state functional magnetic resonance imaging (rs-fMRI), for investigating the structure and function of the brain [15]-[19]. In graph theory-based brain functional network (BFN) analysis, a specific, complex BFN is abstracted onto a network graph composed of node sets and section sets, in which brain regions act as nodes and the structural or functional connection information between two nodes acts as sections [20]. Studying BFNs in this way can reveal mechanisms of action in different brain regions [21]-[23], making it a vital method for investigating the key pathological process of stroke and the mechanism underlying the effect of acupuncture therapy [24] [25].

However, few studies have addressed BFN changes in PSCI patients after acupuncture therapy. This study investigated BFN changes in patients with PSCI after acupuncture therapy via graph theoretical analysis.

2. Materials and Methods

2.1. Clinical Data

In this study, 22 PSCI patients who underwent acupuncture therapy at our hospital were enrolled. The inclusion criteria were as follows: 1) first-onset PSCI and the diagnostic criteria for cerebral infarction, 2) right-handedness, 3) Montreal Cognitive Assessment (MoCA) score < 26 points and Mini-Mental State Examination (MMSE) score < 24 points, and 4) consciousness with stable vital signs. The exclusion criteria were as follows: 1) restroke or hemorrhagic stroke confirmed by imaging; 2) mental illness such as depression, hysteria, or obvious hypophrenia before stroke onset; 3) inability to receive acupuncture therapy or fainting during acupuncture therapy; 4) severe cardiopulmonary or renal dysfunction, blood diseases, or coagulation abnormalities; 5) contraindications to MRI or claustrophobia; and 6) other conditions hindering image acquisition or data quality. All PSCI patients were subjected to the MMSE and MoCA, which were administered by the same experienced neurologist. Fourteen healthy controls (HCs) matched for age, sex, and education level were enrolled in this study. All the subjects signed informed consent forms.

2.2. Rs-fMRI Scan

All the subjects underwent T1-weighted imaging (T1WI) and rs-fMRI scans with a magnetic resonance scanner equipped with a 32-channel head–neck coil (MR750 3.0 T, GE). For PSCI patients, rs-fMRI scans were conducted at baseline and 2 weeks after acupuncture therapy. The T1WI scanning parameters were as follows: repetition time (TR) = 8.2 ms, echo time (TE) = 3.1 ms, field of view (FOV) = 256 × 256 mm, slice thickness = 1 mm, slice increment = 0, matrix = 256 × 256, flip angle = 7˚, and time = 3 min 59 s. The rs-fMRI scanning parameters were as follows: TR = 2000 ms, TE = 30 ms, FOV = 230 × 230 mm, slice thickness = 3.5 mm, slice increment = 0.7 mm, matrix = 64 × 64, flip angle = 90˚, and time = 8 min 10 s.

2.3. Acupuncture Scheme

Acupoints were selected with reference to specific meridians and known acupoints. The acupuncture was performed with disposable sterile 0.35 × 50 mm acupuncture needles as follows. After routine disinfection, the bilateral Neiguan acupoints were first punctured straight to a depth of 20 - 25 mm. After the desired sensation was achieved, the neutral supplementation and draining method was performed, and the needles were twirled 120 times/min continuously for 1 min, after which they were left in place for 30 min. Next, the Baihui and Sishencong acupoints were horizontally punctured to a depth of 20 - 25 mm to reach the galea aponeurotica from front to back. After the desired sensation was achieved, the needles were twirled at a small amplitude and a frequency of 200 times/min continuously for 1 min and then left in place for 30 min. Acupuncture was performed by the same acupuncture therapist at 8:00 - 10:00 in the morning once a day, 5 days a week for a total of 2 weeks.

2.4. Data Processing

The data were preprocessed with the DPABI software package of the MATLAB platform as follows [26]. 1) Data from the first 10 time points were removed to avoid the effects of environmental variations or unstable magnetic fields and ensure signal stability. 2) Time correction was performed by aligning all image layers of each result to the time point in the middle of the scan. 3) Head motion correction was performed, and the data of subjects with head rotation > 2˚ or translation > 2 mm in the *x*-, *y*-, or *z*-directions were excluded. 4) The brain images of each subject were registered to standard Montreal Neurological Institute (MNI) space and then resampled to a voxel size of 3 mm × 3 mm × 3 mm. 5) Linear drift was removed to reduce the baseline drift caused by the machine. 6) Covariates were removed to eliminate the additional effects of head movement, white matter signals, and cerebrospinal fluid signals. 7) All the data were subjected to bandpass filtering between 0.01 and 0.08 Hz to remove high-frequency signals and physiological noise.

2.5. Graph Theoretical Analysis

The brain images of all the subjects were registered to the anatomical automatic labeling (AAL) template with GRETNA on the MATLAB platform [27]. In this template, the whole brain was divided into 90 brain regions, in which each node corresponds to one region. Then, the average time series of all voxels in the 90 brain regions were extracted, and the Pearson correlation coefficients of the average time series between every two brain regions were calculated, yielding a 90 × 90 matrix R. Next, matrix R was subjected to Fisher Z-transformation, yielding a Z value correlation matrix that was almost normally distributed. Network sparsity, the ratio of the number of sections in a network to the maximum number of possible sections in the network, was adopted to determine the BFN thresholds. The lower limit of the threshold should meet the criterion that the average degree of all nodes in a BFN of each subject is greater than 2 log(N), where N is the number of nodes, and the upper limit of the threshold should meet the criterion that the parameter of the small-world topological properties of each BFN is greater than 1.1 [28]. For this reason, the range of sparsity was set to 0.1 - 0.28 in this study, with a step size of 0.01.

The area under the curve (AUC) of the whole-brain topological properties (σ, γ, λ, C_p, L_p, E_{loc}, and E_g) and node properties (betweenness centrality, degree centrality, and nodal local efficiency) in each group was calculated with GRETNA [29]-[31].

2.6. Statistical Analysis

Data analysis was performed with SPSS 25.0 software. The chi-square test and independent-sample *t* test or paired-sample *t* test were employed to compare enumeration data and quantitative data, respectively, between groups. Indicators with differences between groups in terms of whole-brain topological properties and node properties were subjected to Pearson correlation analysis with the MMSE and MoCA scores. For all the statistical results, $p < 0.05$ denoted statistical significance.

3. Results

3.1. Clinical Characteristics

A total of 22 PSCI patients and 14 HCs were included in this study; the demographic and clinical characteristics of the included individuals are shown in **Table 1**. Compared with the pretreatment scores, the posttreatment MMSE and MoCA scores of the PSCI patients were significantly greater (**Table 2**).

Table 1. Clinical characteristics of the PSCI and HC groups.

Clinical characteristics	PSCI	HC	*t*	*p*
Sex (males/females)	11/11	4/10	3.653	0.056
Age (years)	60.1 ± 8.4	56.7 ± 4.6	1.429	0.163
Education level (years)	5.8 ± 3.4	7.7 ± 3.6	0.801	0.132

Table 2. Comparison of clinical scale scores in PSCI patients before and after treatment.

Clinical scale scores	Before treatment	After treatment	*t*	*p*
MMSE	18.14 ± 3.14	22.00 ± 2.60	−5.332	0.000
MoCA	15.91 ± 3.26	20.05 ± 3.36	−7.343	0.000

Notes: MMSE: Mini-Mental State Examination. MoCA: Montreal Cognitive Assessment.

3.2. Global Topological Properties

Small-world network attributes were observed in both groups for sparsity values between 0.1 and 0.28. Compared with HCs, PSCI patients had decreased values for the network metric γ ($p = 0.024$), the clustering coefficient (C_p) ($p = 0.038$), and E_{loc} ($p = 0.025$).

3.3. Comparison of Nodal Attributes

3.3.1. Betweenness Centrality

The betweenness centrality in the left cuneus (CUN. L) and right Heschl's gyrus (HES. R) was greater in PSCI patients than in HCs over the entire threshold range ($p < 0.05$) (Table 3 and Figure 1). After treatment, PSCI patients had lower betweenness centrality in the PCG.L and CUN. L ($p < 0.05$) (Table 4 and Figure 1).

Table 3. Comparison of topological properties between PSCI patients before treatment and HCs.

Parameters	Brain region	MNI coordinate			Control group	PSCI patients	*t*	*p*
		X	*y*	*z*				
BC	CUN. L	−5.93	−80.13	27.22	3.01 ± 1.99	9.77 ± 8.94	−2.568	0.002
	HES. R	45.86	−17.15	10.41	2.52 ± 1.79	6.80 ± 6.36	−2.615	0.003
DC	SFGdor. L	−18.45	34.81	42.2	1.88 ± 0.84	2.92 ± 1.44	−2.292	0.029
	MFG. R	37.59	33.06	34.04	4.68 ± 1.54	3.09 ± 1.48	2.970	0.006
	IFGoperc. R	50.2	14.98	21.41	3.52 ± 1.69	2.30 ± 1.28	2.353	0.025
	PCG. L	−4.85	−42.92	24.67	2.37 ± 1.64	3.56 ± 1.63	−2.042	0.049
	SOG. R	−32.39	−80.73	16.11	5.20 ± 0.95	3.93 ± 1.51	2.635	0.005
	IPL. L	−42.8	−45.82	46.74	3.18 ± 1.57	4.30 ± 1.34	−2.194	0.036
	HES. R	−45.86	−17.15	10.41	1.42 ± 0.96	2.43 ± 1.21	−2.483	0.018
NLE	ORBsup. R	18.49	48.10	−14.02	0.11 ± 0.03	0.14 ± 0.01	−3.853	0.005
	ORBsupmed. R	8.16	51.67	−7.13	0.13 ± 0.02	0.14 ± 0.02	−2.039	0.049
	DCG. L	−5.48	−14.92	41.57	0.13 ± 0.03	0.15 ± 0.01	−2.830	0.008
	SMG. R	57.61	−31.50	34.48	0.12 ± 0.05	0.15 ± 0.01	−2.276	0.030
	TPOsup. L	−39.88	15.14	−20.18	0.11 ± 0.03	0.14 ± 0.02	−2.582	0.014

Notes: BC: Betweenness centrality. DC: Degree centrality. NLE: Nodal local efficiency. PSCI: poststroke cognitive impairment. IPL. L: left inferior parietal but supramarginal and angular gyrus. PCG. L: left posterior cingulate gyrus. HES. R: right Heschl's gyrus. SOG. R: right superior occipital gyrus. IFGoperc. R: right inferior frontal gyrus, pars opercularis. MFG. R: right middle frontal gyrus. CUN. L: left cuneus. ORBsupmed. R: right superior frontal gyrus, pars medialis orbitalis. ORBsup. R: right superior frontal gyrus, pars orbitalis. DCG. L: left median cingulate and paracingulate gyri. SMG. R: right supramarginal gyrus. TPOsup. L: left temporal pole: superior temporal gyrus.

Table 4. Comparison of topological properties in PSCI patients before and after treatment.

Parameters	Brain region	MNI coordinate			Before treatment	After treatment	*t*	*p*
		x	*y*	*z*				
BC	PCG. L	−4.85	−42.92	24.67	10.36 ± 8.34	6.13 ± 5.45	2.475	0.022
	CUN. L	−5.93	−80.13	27.22	9.77 ± 8.94	4.99 ± 4.63	2.337	0.029
DC	ORBsupmed. R	8.16	51.67	−7.13	2.70 ± 1.31	2.04 ± 1.06	2.513	0.020
	LING. L	−14.62	−67.56	−4.63	3.79 ± 1.48	4.78 ± 1.43	−2.717	0.013
	LING. R	16.29	−66.93	−3.87	3.91 ± 1.36	4.73 ± 1.11	−2.298	0.032
	IOG. L	−36.36	−78.29	−7.84	2.83 ± 1.68	3.78 ± 1.46	−2.148	0.044
NLE	PHG. L	−21.17	−15.95	−20.70	0.12 ± 0.05	0.15 ± 0.01	−2.278	0.034
	IOG. R	38.16	−81.99	−7.61	0.14 ± 0.02	0.16 ± 0.01	−2.960	0.008
	FFG. L	−31.16	−40.30	−20.23	0.13 ± 0.02	0.14 ± 0.01	−2.140	0.043
	ANG. R	45.51	−59.98	38.63	0.15 ± 0.01	0.13 ± 0.04	2.426	0.025
	HES. L	−41.99	−18.88	9.98	0.14 ± 0.02	0.15 ± 0.01	−2.911	0.009

Notes: BC: betweenness centrality. DC: degree centrality. NLE: Nodal local efficiency. PSCI: poststroke cognitive impairment. SFGdor.L: left superior frontal gyrus, dorsolateral. IPL. L: left Inferior parietal, but supramarginal and angular gyri. PCG. L: left posterior cingulate gyrus. HES. R: right Heschl's gyrus. SOG. R: right superior occipital gyrus. IFGoperc. R: right inferior frontal gyrus, pars opercularis. CUN. L: left cuneus. HES. L: left Heschl's gyrus. PHG. L: parahippocampal gyrus. FFG. L: fusiform gyrus. IOG. R: inferior occipital gyrus. ANG. R: angular gyrus. IOG. L: left inferior occipital gyrus. LING. R: right lingual gyrus. ORBsupmed. R: right superior frontal gyrus, pars medialis orbitalis. LING. L: left lingual gyrus.

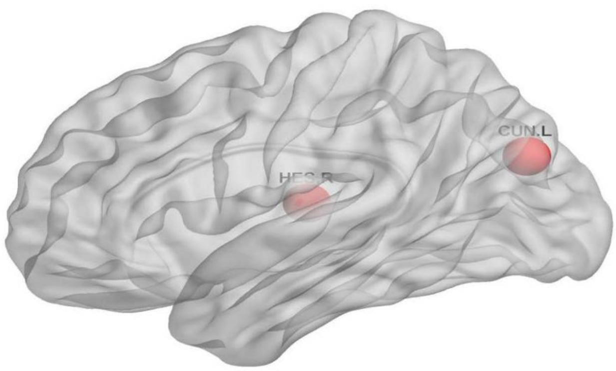

(a)

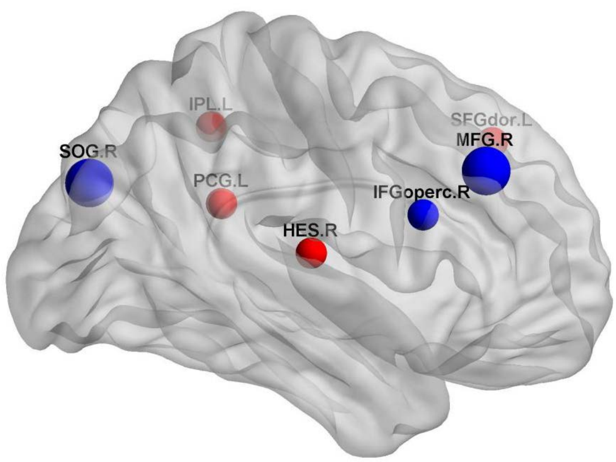

(b)

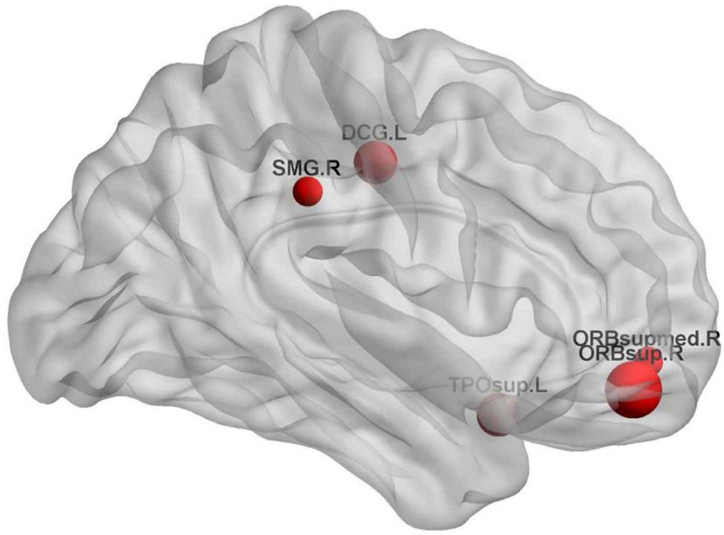
DCG.L
SMG.R
ORBsupmed.R
ORBsup.R
TPOsup.L

(c)

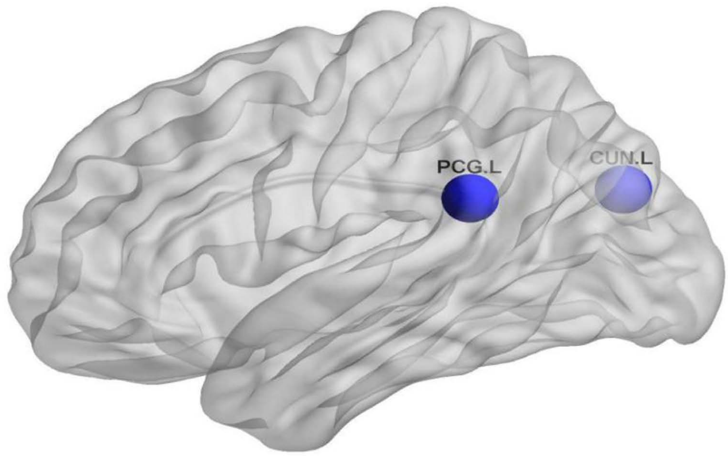
PCG.L
CUN.L

(d)

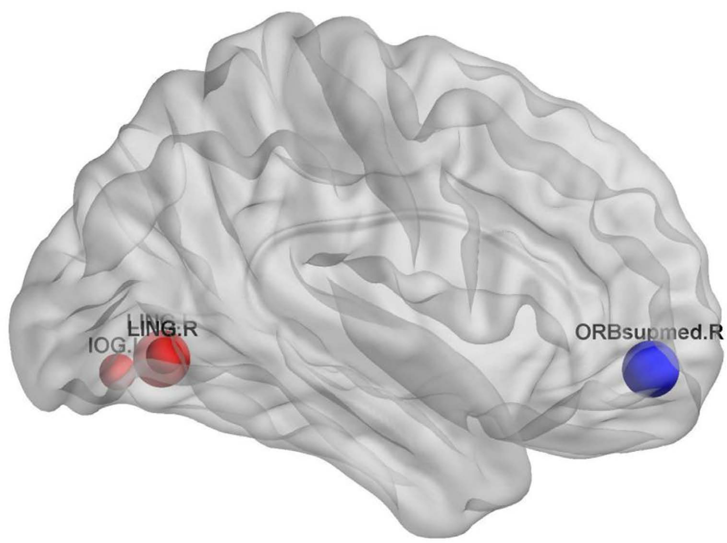
LING.R
ORBsupmed.R

(e)

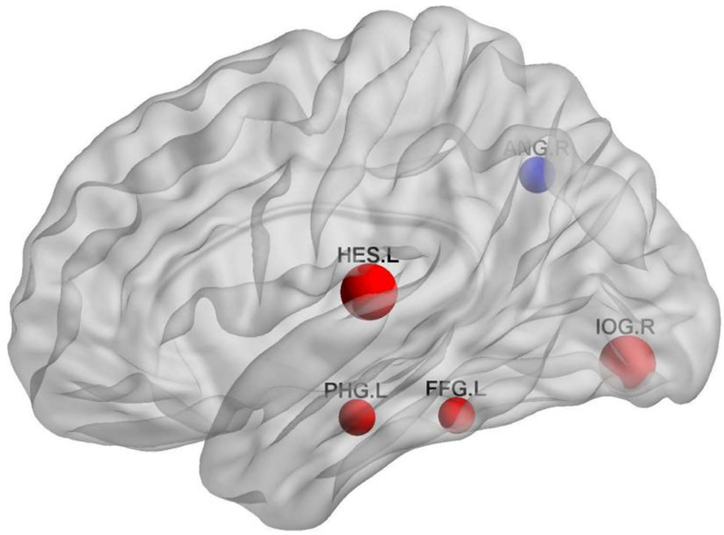

(f)

Note: Red nodes are brain regions with increases, and blue nodes are brain regions with decreases in the above values. The size of each node represents its t value. PSCI: poststroke cognitive impairment. SFGdor. L: left superior frontal gyrus, dorsolateral. IPL. L: left inferior parietal but supramarginal and angular gyri. PCG. L: left posterior cingulate gyrus. HES. R: right Heschl's gyrus. SOG. R: right superior occipital gyrus. IFGoperc. R: right inferior frontal gyrus, pars opercularis. MFG. R: right middle frontal gyrus. CUN. L: left cuneus. HES. L: left Heschl's gyrus. PHG. L: parahippocampal gyrus. FFG. L: Fusiform gyrus. IOG. R: inferior occipital gyrus. ANG. R: angular gyrus. IOG. L: left inferior occipital gyrus. LING. R: right lingual gyrus. ORBsupmed. R: right superior frontal gyrus, pars medialis orbitalis. ORBsup. R: right superior frontal gyrus, pars orbitalis. DCG. L: left median cingulate and paracingulate gyri. SMG. R: right supramarginal gyrus. TPOsup. L: left temporal pole: superior temporal gyrus. LING. L: left lingual gyrus.

Figure 1. Altered brain regions between groups. (a) The betweenness centrality in the CUN. L and the HES. R was greater in PSCI patients than in HCs. (b) The degree centrality in the SFGdor. L, PCG.L, IPL. L, and HES. R was greater in PSCI patients than in HCs, whereas that in the MFG. R, IFGoperc. R, and SOG. R was lower in PSCI patients than in HCs. (c) Nodal local efficiency in the ORBsup.R, ORBsupmed.R, DCG. L, SMG. R, and TPOsup. L was greater in PSCI patients than in HCs. (d) PSCI patients had lower betweenness centrality in the PCG. L and CUN. L. (e) The degree centrality in the LING. L, LING. R, and IOG. L increased after treatment in PSCI patients, whereas that in the ORBsupmed. R declined. (f) Nodal local efficiency in the PHG. L, IOG. R, FFG. L, and HES. L was elevated, whereas that in the ANG. R was decreased in PSCI patients after treatment.

3.3.2. Degree Centrality

The degree centrality in the left dorsal superior frontal gyrus (SFGdor. L), PCG. L, left inferior parietal lobe (IPL. L), and the HES. R was greater in PSCI patients than in HCs, whereas that in the right medial frontal gyrus (MFG. R), right inferior frontal gyrus, pars opercularis (IFGoperc.R), and right superior occipital gyrus (SOG.R) was lower in PSCI patients than in HCs ($p < 0.05$) (**Table 3** and **Figure 1**).

Compared with that before treatment, the degree centrality in the left lingual gyrus (LING. L), right lingual gyrus (LING.R), and left inferior occipital gyrus

(IOG. L) was increased, whereas in the right superior frontal gyrus, pars medialis orbitalis (ORBsupmed. R) was decreased after treatment in PSCI patients (p < 0.05) (**Table 4** and **Figure 1**).

3.3.3. Nodal Local Efficiency

The nodal local efficiency in the right superior frontal gyrus, pars orbitalis (ORBsup. R), ORBsupmed. R, left median cingulate and paracingulate gyri (DCG. L), SMG. R, and left temporal pole: superior temporal gyrus (TPOsup. L) was greater in PSCI patients than in HCs (p < 0.05) (**Table 3** and **Figure 1**).

Compared with that before treatment, the nodal local efficiency in the left parahippocampal gyrus (PHG. L), IOG. R, left fusiform gyrus (FFG. L), and the HES. L was elevated, whereas that in the right angular gyrus (ANG. R) was lower in PSCI patients after treatment (p < 0.05) (**Table 4** and **Figure 1**).

3.4. Relationships between BFN Indicators and Clinical Scale Scores

The AUC of the nodal local efficiency in the ORBsupmed. R in PSCI patients before treatment was positively correlated with the MoCA score (r = 0.463, p = 0.042), whereas the AUC of the degree centrality in the IOG. L after acupuncture therapy was negatively associated with the MoCA score (r = −0.461, p = 0.031).

4. Discussion

Small-world properties are the basic topological organizational attributes of the human brain [32]-[36]. The small-world network is a state between a regular network and a random network [37]-[39]. In patients with certain diseases, BFN attributes maintain small-world characteristics [32]-[39]. The BFNs of PSCI patients deviate from the low-cost and efficient operation mode of normal BFNs, in which a balance between functional separation and functional integration is necessary to ensure optimal operation [40]-[44]. In the present study, small-world properties were observed in both the PSCI patient and HC groups, and the C_p, γ, and E_{loc} values were lower in the PSCI patients before treatment than in the HCs. The results of the present study are in line with those of the above studies. We speculate that the balance between the functional separation and functional integration of BFNs in PSCI patients is disturbed, manifesting mainly as altered functional separation, which results in cognitive decline [44].

This study revealed that the abnormal node centrality in the BFNs of PSCI patients involved mainly the default mode network (DMN) and the executive control network (ECN). A previous study indicated that the DMN and ECN are related to cognitive function [45]-[52]. Our findings suggest that alterations in these brain regions might exert crucial effects on the BFNs of PSCI patients. The results of this study also revealed that node centrality in several brain regions involving the occipital lobe was elevated in PSCI patients after acupuncture therapy compared with before treatment. The occipital lobe is involved mainly in the visual processing of information, whereas the lingual gyrus is also involved in word processing. Zhang *et al.* analyzed fMRI data and discovered that the degree of activation of the LING. L is positively correlated with the performance of activities related to semantic processing [53]. In some Alzheimer's disease patients, visual cognitive dysfunction is related to occipital atrophy [54]. In the present study, PSCI patients had increased node centrality in the bilateral LING and the IOG. L after treatment, indicating that acupuncture therapy likely improves cognitive functions related to visual space and language. The greater local efficiency of nodes in all differential brain regions in our PSCI patients before treatment than in the normal controls may reflect a compensatory mechanism, *i.e.*, compensation for functional connectivity loss between distant brain regions via an increase in the number of connections with adjacent brain regions [55]. In addition, the nodal local efficiency in the PHG. L, IOG.R, FFG. L, and HES. L was elevated, whereas that in the ANG. R was lowered after treatment in PSCI patients. Such alterations in these brain regions are associated with cognitive tasks, including memory, language, vision, and hearing [56] [57]. One study implicated cognitive impairment in the reduced nodal efficiency in the temporal/parietal lobe of patients with subcortical ischemic cerebrovascular disease and cognitive impairment [58]. The results of this study revealed that the local efficiency of cognition-related nodes was increased in PSCI patients after treatment, which may indicate that acupuncture may improve the cognitive function of these patients.

Published studies have shown that acupuncture can exert beneficial effects on PSCI [3]-[14]. In the present study, the posttreatment MMSE and MoCA scores of the PSCI patients were significantly greater than the pretreatment scores were. The mechanisms of acupuncture for PSCI may involve antineuronal apoptosis, the promotion of synaptic plasticity, the regulation of brain energy metabolism disorders, etc. [12] [59]. Acupuncture is recommended by the World Health Organization as an alternative and complementary strategy for improving stroke care. However, acupuncture combined with routine therapy is widely used in clinical practice to ensure optimal effects [60] [61]. In the present study, only basic therapies were combined.

The present study had the following limitations: 1) The enrolled PSCI patients had mild cognitive impairment, and we did not quantify BFN differences between patients with different degrees of cognitive impairment. 2) The topological properties of BFNs are affected by the template used [62]. In this study, the classical AAL90 brain atlas was employed as part of the segmentation strategy. In the future, the effects of other templates, such as the AAL116 brain atlas and the Dosenbach 160 brain atlas, should be explored to validate the results. 3) A sham acupuncture group should be established to conduct more complete controlled experiments in future research. In addition, PSCI patients were provided acupuncture treatment 3 - 5 times per week for 4 - 12 weeks in many previous studies [10] [63]. For various reasons, the PSCI patients in this study were discharged after receiving acupuncture treatment for only two weeks. This study needs to be further improved in the future.

5. Conclusion

The results of this study indicate that the cognitive decline in PSCI patients may be related to BFN disorders and that acupuncture therapy may modulate the topological properties of the BFNs of PSCI patients.

Author Contributions

Conception, X.-H.H., L.Y., X.-M.Z.; patient recruitment and exploration, R.W., N.L., H.X., P.Z.; data analysis, R.W., N.L.; manuscript writing and revision, R.W., P. Z., L.Y.; All authors have read and agreed to the published version of the manuscript.

Funding

This work was supported by the Project of Scientific Research Development Plan of the Affiliated Hospital of North Sichuan Medical College (No. 2020ZD017; 2020ZD008).

Ethics Statement

This study was approved by the Ethics Committee of the Affiliated Hospital of North Sichuan Medical College (No. 2020ER117-1).

Informed Consent Statement

Informed consent was obtained from all the subjects involved in the study.

Data Availability Statement

The original contributions presented in the study are included in the article. Further inquiries can be directed to the corresponding author.

Conflicts of Interest

The authors declare that they have no conflicts of interest.

References

[1] Qu, Y., Zhuo, L., Li, N., Hu, Y., Chen, W., Zhou, Y., *et al*. (2015) Prevalence of Post-Stroke Cognitive Impairment in China: A Community-Based, Cross-Sectional Study. *PLOS ONE*, **10**, e0122864. https://doi.org/10.1371/journal.pone.0122864

[2] Deramecourt, V. and Pasquier, F. (2014) Neuronal Substrate of Cognitive Impairment in Post-Stroke Dementia. *Brain*, **137**, 2404-2405. https://doi.org/10.1093/brain/awu188

[3] Taya, F., Sun, Y., Babiloni, F., Thakor, N. and Bezerianos, A. (2015) Brain Enhancement through Cognitive Training: A New Insight from Brain Connectome. *Frontiers in Systems Neuroscience*, **9**, Article 44. https://doi.org/10.3389/fnsys.2015.00044

[4] Sun, P.Y., Cai, R.L., Li, P.F., Zhu, Y., Wang, T., Wu, J., Li, N., Liu, H. and Chu, H.R. (2019) Protective Effects on Hippocampal Neurons and the Influence on Hippocampal Monoamine Neurotransmitters with Acupuncture for Promoting the Circulation

of the Governor Vessel and Regulating the Mental State in Rats with Post-Stroke Depression. *Chinese Acupuncture & Moxibustion*, **39**, 741-747.

[5] Chavez, L., Huang, S., MacDonald, I., Lin, J., Lee, Y. and Chen, Y. (2017) Mechanisms of Acupuncture Therapy in Ischemic Stroke Rehabilitation: A Literature Review of Basic Studies. *International Journal of Molecular Sciences*, **18**, Article 2270. https://doi.org/10.3390/ijms18112270

[6] Peng, J., Su, J., Song, L., Lv, Q., Gao, Y., Chang, J., *et al.* (2023) Altered Functional Activity and Functional Connectivity of Seed Regions Based on ALFF Following Acupuncture Treatment in Patients with Stroke Sequelae with Unilateral Limb Numbness [Corrigendum]. *Neuropsychiatric Disease and Treatment*, **19**, 367-368. https://doi.org/10.2147/ndt.s408402

[7] Liu, F., Hou, Y., Chen, X., Chen, Z., Su, G. and Lin, R. (2024) Moxibustion Promoted Axonal Regeneration and Improved Learning and Memory of Post-Stroke Cognitive Impairment by Regulating PI_3K/AKt and $TACC_3$. *Neuroscience*, **551**, 299-306. https://doi.org/10.1016/j.neuroscience.2024.05.027

[8] Li, Z.T., Ban, L.Q. and Chen, F. (2023) Acupuncture of Revised Acupoint Combination around the Skull Base for Post-Stroke Mild Cognitive Impairment: A Randomized Controlled Trial. *Chinese Acupuncture & Moxibustion*, **43**, 1104-1108.

[9] Zhou, Q., Ji, Y., Lv, Y., Xue, J., Wang, Y. and Huang, Y. (2023) Scientific Evidence of Acupuncture for Post-Stroke Cognitive Impairment: An Overview of Systematic Reviews and Meta-Analyses. *Neuropsychiatric Disease and Treatment*, **19**, 1503-1513. https://doi.org/10.2147/ndt.s407162

[10] Li, L., Yang, L., Luo, B., Deng, L., Zhong, Y., Gan, D., *et al.* (2022) Acupuncture for Post-Stroke Cognitive Impairment: An Overview of Systematic Reviews. *International Journal of General Medicine*, **15**, 7249-7264. https://doi.org/10.2147/ijgm.s376759

[11] Zhuo, P., Huang, L., Lin, M., Chen, J., Dai, Y., Yang, M., *et al.* (2023) Efficacy and Safety of Acupuncture Combined with Rehabilitation Training for Poststroke Cognitive Impairment: A Systematic Review and Meta-Analysis. *Journal of Stroke and Cerebrovascular Diseases*, **32**, Article 107231. https://doi.org/10.1016/j.jstrokecerebrovasdis.2023.107231

[12] Li, N., Wang, H., Liu, H., Zhu, L., Lyu, Z., Qiu, J., *et al.* (2023) The Effects and Mechanisms of Acupuncture for Post-Stroke Cognitive Impairment: Progress and Prospects. *Frontiers in Neuroscience*, **17**, Article 1211044. https://doi.org/10.3389/fnins.2023.1211044

[13] Liu, Y., Chen, F., Qin, P., Zhao, L., Li, X., Han, J., *et al.* (2023) Acupuncture Treatment Vs. Cognitive Rehabilitation for Post-Stroke Cognitive Impairment: A Systematic Review and Meta-Analysis of Randomized Controlled Trials. *Frontiers in Neurology*, **14**, Article 1035125. https://doi.org/10.3389/fneur.2023.1035125

[14] Huang, J., You, X., Liu, W., Song, C., Lin, X., Zhang, X., *et al.* (2017) Electroacupuncture Ameliorating Post-Stroke Cognitive Impairments via Inhibition of Peri-Infarct Astroglial and Microglial/Macrophage P2 Purinoceptors-Mediated Neuroinflammation and Hyperplasia. *BMC Complementary and Alternative Medicine*, **17**, Article No. 480. https://doi.org/10.1186/s12906-017-1974-y

[15] He, Y. and Evans, A. (2014) Magnetic Resonance Imaging of Healthy and Diseased Brain Networks. *Frontiers in Human Neuroscience*, **8**, Article 890. https://doi.org/10.3389/fnhum.2014.00890

[16] Wang, H., Huang, Y., Li, M., Yang, H., An, J., Leng, X., *et al.* (2022) Regional Brain Dysfunction in Insomnia after Ischemic Stroke: A Resting-State fMRI Study. *Frontiers*

in Neurology, **13**, Article 1025174. https://doi.org/10.3389/fneur.2022.1025174

[17] Wang, R., Liu, N., Tao, Y., Gong, X., Zheng, J., Yang, C., *et al.* (2020) The Application of rs-fMRI in Vascular Cognitive Impairment. *Frontiers in Neurology*, **11**, Article 951. https://doi.org/10.3389/fneur.2020.00951

[18] Wei, B., Huang, X., Ji, Y., Fu, W., Cheng, Q., Shu, B., *et al.* (2024) Analyzing the Topological Properties of Resting-State Brain Function Network Connectivity Based on Graph Theoretical Methods in Patients with High Myopia. *BMC Ophthalmology*, **24**, Article No. 315. https://doi.org/10.1186/s12886-024-03592-6

[19] Liu, X., Qiu, S., Wang, X., Chen, H., Tang, Y. and Qin, Y. (2023) Aberrant Dynamic Functional-Structural Connectivity Coupling of Large-Scale Brain Networks in Poststroke Motor Dysfunction. *NeuroImage: Clinical*, **37**, Article 103332. https://doi.org/10.1016/j.nicl.2023.103332

[20] Yin, D., Song, F., Xu, D., Sun, L., Men, W., Zang, L., *et al.* (2013) Altered Topological Properties of the Cortical Motor-Related Network in Patients with Subcortical Stroke Revealed by Graph Theoretical Analysis. *Human Brain Mapping*, **35**, 3343-3359. https://doi.org/10.1002/hbm.22406

[21] Bullmore, E. and Sporns, O. (2009) Complex Brain Networks: Graph Theoretical Analysis of Structural and Functional Systems. *Nature Reviews Neuroscience*, **10**, 186-198. https://doi.org/10.1038/nrn2575

[22] Boot, E.M., Omes, Q.P.M., Maaijwee, N., Schaapsmeerders, P., Arntz, R.M., Rutten-Jacobs, L.C.A., *et al.* (2023) Functional Brain Connectivity in Young Adults with Post-Stroke Epilepsy. *Brain Communications*, **5**, fcad277. https://doi.org/10.1093/braincomms/fcad277

[23] Zhang, T., Liao, Q., Zhang, D., Zhang, C., Yan, J., Ngetich, R., *et al.* (2021) Predicting MCI to AD Conversation Using Integrated sMRI and rs-Fmri: Machine Learning and Graph Theory Approach. *Frontiers in Aging Neuroscience*, **13**, Article 688926. https://doi.org/10.3389/fnagi.2021.688926

[24] Rao, B., Wang, S., Yu, M., Chen, L., Miao, G., Zhou, X., *et al.* (2022) Suboptimal States and Frontoparietal Network-Centered Incomplete Compensation Revealed by Dynamic Functional Network Connectivity in Patients with Post-Stroke Cognitive Impairment. *Frontiers in Aging Neuroscience*, **14**, Article 893297. https://doi.org/10.3389/fnagi.2022.893297

[25] Xu, M., Qian, L., Wang, S., Cai, H., Sun, Y., Thakor, N., *et al.* (2023) Brain Network Analysis Reveals Convergent and Divergent Aberrations between Mild Stroke Patients with Cortical and Subcortical Infarcts during Cognitive Task Performing. *Frontiers in Aging Neuroscience*, **15**, Article 1193292. https://doi.org/10.3389/fnagi.2023.1193292

[26] Yan, C., Wang, X., Zuo, X. and Zang, Y. (2016) DPABI: Data Processing & Analysis for (Resting-State) Brain Imaging. *Neuroinformatics*, **14**, 339-351. https://doi.org/10.1007/s12021-016-9299-4

[27] Tzourio-Mazoyer, N., Landeau, B., Papathanassiou, D., Crivello, F., Etard, O., Delcroix, N., *et al.* (2002) Automated Anatomical Labeling of Activations in SPM Using a Macroscopic Anatomical Parcellation of the MNI MRI Single-Subject Brain. *NeuroImage*, **15**, 273-289. https://doi.org/10.1006/nimg.2001.0978

[28] Yu, M., Dai, Z., Tang, X., Wang, X., Zhang, X., Sha, W., *et al.* (2017) Convergence and Divergence of Brain Network Dysfunction in Deficit and Non-Deficit Schizophrenia. *Schizophrenia Bulletin*, **43**, 1315-1328. https://doi.org/10.1093/schbul/sbx014

[29] Fornito, A., Zalesky, A. and Breakspear, M. (2013) Graph Analysis of the Human

Connectome: Promise, Progress, and Pitfalls. *NeuroImage*, **80**, 426-444. https://doi.org/10.1016/j.neuroimage.2013.04.087

[30] Watts, D.J. and Strogatz, S.H. (1998) Collective Dynamics of 'Small-World' Networks. *Nature*, **393**, 440-442. https://doi.org/10.1038/30918

[31] Humphries, M.D., Gurney, K. and Prescott, T.J. (2005) The Brainstem Reticular Formation Is a Small-World, Not Scale-Free, Network. *Proceedings of the Royal Society B: Biological Sciences*, **273**, 503-511. https://doi.org/10.1098/rspb.2005.3354

[32] Wang, Z., Yuan, Y., Bai, F., You, J. and Zhang, Z. (2016) Altered Topological Patterns of Brain Networks in Remitted Late-Onset Depression. *The Journal of Clinical Psychiatry*, **77**, 123-130. https://doi.org/10.4088/jcp.14m09344

[33] Tao, Y., Ficek, B., Rapp, B. and Tsapkini, K. (2020) Different Patterns of Functional Network Reorganization across the Variants of Primary Progressive Aphasia: A Graph-Theoretic Analysis. *Neurobiology of Aging*, **96**, 184-196. https://doi.org/10.1016/j.neurobiolaging.2020.09.007

[34] He, S., Liu, Z., Xu, Z., Duan, R., Yuan, L., Xiao, C., *et al.* (2020) Brain Functional Network in Chronic Asymptomatic Carotid Artery Stenosis and Occlusion: Changes and Compensation. *Neural Plasticity*, **2020**, 1-11. https://doi.org/10.1155/2020/9345602

[35] Bahrami, N., Seibert, T.M., Karunamuni, R., Bartsch, H., Krishnan, A., Farid, N., *et al.* (2017) Altered Network Topology in Patients with Primary Brain Tumors after Fractionated Radiotherapy. *Brain Connectivity*, **7**, 299-308. https://doi.org/10.1089/brain.2017.0494

[36] Wang, J., Chen, Y., Liang, H., Niedermayer, G., Chen, H., Li, Y., *et al.* (2019) The Role of Disturbed Small-World Networks in Patients with White Matter Lesions and Cognitive Impairment Revealed by Resting State Function Magnetic Resonance Images (rs-fMRI). *Medical Science Monitor*, **25**, 341-356. https://doi.org/10.12659/msm.913396

[37] Telesford, Q.K., Joyce, K.E., Hayasaka, S., Burdette, J.H. and Laurienti, P.J. (2011) The Ubiquity of Small-World Networks. *Brain Connect*, **1**, 367-375. https://doi.org/10.1089/brain.2011.0038

[38] Bullmore, E.T. and Bassett, D.S. (2011) Brain Graphs: Graphical Models of the Human Brain Connectome. *Annual Review of Clinical Psychology*, **7**, 113-140. https://doi.org/10.1146/annurev-clinpsy-040510-143934

[39] Wang, Q., Su, T., Zhou, Y., Chou, K., Chen, I., Jiang, T., *et al.* (2012) Anatomical Insights into Disrupted Small-World Networks in Schizophrenia. *NeuroImage*, **59**, 1085-1093. https://doi.org/10.1016/j.neuroimage.2011.09.035

[40] Zhu, Y., Bai, L., Liang, P., Kang, S., Gao, H. and Yang, H. (2016) Disrupted Brain Connectivity Networks in Acute Ischemic Stroke Patients. *Brain Imaging and Behavior*, **11**, 444-453. https://doi.org/10.1007/s11682-016-9525-6

[41] Shi, M., Liu, S., Chen, H., Geng, W., Yin, X., Chen, Y., *et al.* (2020) Disrupted Brain Functional Network Topology in Unilateral Acute Brainstem Ischemic Stroke. *Brain Imaging and Behavior*, **15**, 444-452. https://doi.org/10.1007/s11682-020-00353-z

[42] Xu, J., Chen, F., Lei, D., Zhan, W., Sun, X., Suo, X., *et al.* (2018) Disrupted Functional Network Topology in Children and Adolescents with Post-Traumatic Stress Disorder. *Frontiers in Neuroscience*, **12**, Article 709. https://doi.org/10.3389/fnins.2018.00709

[43] Siegel, J.S., Seitzman, B.A., Ramsey, L.E., Ortega, M., Gordon, E.M., Dosenbach, N.U.F., *et al.* (2018) Re-Emergence of Modular Brain Networks in Stroke Recovery.

Cortex, **101**, 44-59. https://doi.org/10.1016/j.cortex.2017.12.019

[44] Yu, Y., Zhou, X., Wang, H., Hu, X., Zhu, X., Xu, L., *et al.* (2015) Small-World Brain Network and Dynamic Functional Distribution in Patients with Subcortical Vascular Cognitive Impairment. *PLOS ONE*, **10**, e0131893. https://doi.org/10.1371/journal.pone.0131893

[45] Liu, Y., Yang, K., Hu, X., Xiao, C., Rao, J., Li, Z., *et al.* (2020) Altered Rich-Club Organization and Regional Topology Are Associated with Cognitive Decline in Patients with Frontal and Temporal Gliomas. *Frontiers in Human Neuroscience*, **14**, Article 23. https://doi.org/10.3389/fnhum.2020.00023

[46] Zuo, X., Ehmke, R., Mennes, M., Imperati, D., Castellanos, F.X., Sporns, O., *et al.* (2011) Network Centrality in the Human Functional Connectome. *Cerebral Cortex*, **22**, 1862-1875. https://doi.org/10.1093/cercor/bhr269

[47] Rubinov, M. and Sporns, O. (2010) Complex Network Measures of Brain Connectivity: Uses and Interpretations. *NeuroImage*, **52**, 1059-1069. https://doi.org/10.1016/j.neuroimage.2009.10.003

[48] Zhu, Y., Lu, T., Xie, C., Wang, Q., Wang, Y., Cao, X., *et al.* (2020) Functional Disorganization of Small-World Brain Networks in Patients with Ischemic Leukoaraiosis. *Frontiers in Aging Neuroscience*, **12**, Article 203. https://doi.org/10.3389/fnagi.2020.00203

[49] Fransson, P. and Marrelec, G. (2008) The Precuneus/Posterior Cingulate Cortex Plays a Pivotal Role in the Default Mode Network: Evidence from a Partial Correlation Network Analysis. *NeuroImage*, **42**, 1178-1184. https://doi.org/10.1016/j.neuroimage.2008.05.059

[50] Zhang, J., Zhang, Y., Wang, L., Sang, L., Yang, J., Yan, R., *et al.* (2017) Disrupted Structural and Functional Connectivity Networks in Ischemic Stroke Patients. *Neuroscience*, **364**, 212-225. https://doi.org/10.1016/j.neuroscience.2017.09.009

[51] Li, Q., Liu, J., Wang, W., Wang, Y., Li, W., Chen, J., *et al.* (2018) Disrupted Coupling of Large-Scale Networks Is Associated with Relapse Behaviour in Heroin-Dependent Men. *Journal of Psychiatry & Neuroscience*, **43**, 48-57. https://doi.org/10.1503/jpn.170011

[52] Seeley, W.W., Menon, V., Schatzberg, A.F., Keller, J., Glover, G.H., Kenna, H., *et al.* (2007) Dissociable Intrinsic Connectivity Networks for Salience Processing and Executive Control. *The Journal of Neuroscience*, **27**, 2349-2356. https://doi.org/10.1523/jneurosci.5587-06.2007

[53] Zhang, H., Liu, J. and Zhang, Q. (2014) Neural Representations for the Generation of Inventive Conceptions Inspired by Adaptive Feature Optimization of Biological Species. *Cortex*, **50**, 162-173. https://doi.org/10.1016/j.cortex.2013.01.015

[54] Putcha, D., Brickhouse, M., Touroutoglou, A., Collins, J.A., Quimby, M., Wong, B., *et al.* (2019) Visual Cognition in Non-Amnestic Alzheimer's Disease: Relations to Tau, Amyloid, and Cortical Atrophy. *NeuroImage: Clinical*, **23**, Article 101889. https://doi.org/10.1016/j.nicl.2019.101889

[55] Mijalkov, M., Kakaei, E., Pereira, J.B., Westman, E. and Volpe, G. (2017) BRAPH: A Graph Theory Software for the Analysis of Brain Connectivity. *PLOS ONE*, **12**, e178798.

[56] Baldassano, C., Beck, D.M. and Fei-Fei, L. (2013) Differential Connectivity within the Parahippocampal Place Area. *NeuroImage*, **75**, 228-237. https://doi.org/10.1016/j.neuroimage.2013.02.073

[57] Weiner, K.S. and Zilles, K. (2016) The Anatomical and Functional Specialization of the Fusiform Gyrus. *Neuropsychologia*, **83**, 48-62.

https://doi.org/10.1016/j.neuropsychologia.2015.06.033

[58] Sang, L., Chen, L., Wang, L., Zhang, J., Zhang, Y., Li, P., *et al*. (2018) Progressively Disrupted Brain Functional Connectivity Network in Subcortical Ischemic Vascular Cognitive Impairment Patients. *Frontiers in Neurology*, **9**, Article 94. https://doi.org/10.3389/fneur.2018.00094

[59] Cabioglu, M.T. (2016) Acupuncture Practices and Brain Waves. *Open Access Library*, **3**, 1-4. https://doi.org/10.4236/oalib.1102639

[60] Wu, W., Song, C., Yang, Y., Hu, Y. and Lin, H. (2024) Acupuncture for Cognitive Impairment after Stroke: A Systematic Review and Meta-Analysis. *Heliyon*, **10**, e30522. https://doi.org/10.1016/j.heliyon.2024.e30522

[61] Wang, Z., Sun, Z., Zhang, M., Xiong, K. and Zhou, F. (2022) Systematic Review and Meta-Analysis of Acupuncture in the Treatment of Cognitive Impairment after Stroke. *Medicine*, **101**, e30461. https://doi.org/10.1097/md.0000000000030461

[62] Wang, J., Wang, L., Zang, Y., Yang, H., Tang, H., Gong, Q., *et al*. (2008) Parcellation-Dependent Small-World Brain Functional Networks: A Resting-State fMRI Study. *Human Brain Mapping*, **30**, 1511-1523. https://doi.org/10.1002/hbm.20623

[63] Du, Y., Zhang, L., Liu, W., Rao, C., Li, B., Nan, X., *et al*. (2020) Effect of Acupuncture Treatment on Post-Stroke Cognitive Impairment. *Medicine*, **99**, e23803. https://doi.org/10.1097/md.0000000000023803